Journal of Geoscience and Environment Protection, 2024, 12, 270-287
https://www.scirp.org/journal/gep
ISSN Online: 2327-4344
ISSN Print: 2327-4336

Effects of Matter in Atmospheric Neutrino Oscillations and the Formation of Magma

Guowen Zhang*, **Mengke Zhang**

Wuhan Neutrino Science & Technology Co., Ltd., Wuhan, China
Email: *gwz1000@sina.com

How to cite this paper: Zhang, G. W., & Zhang, M. K. (2024). Effects of Matter in Atmospheric Neutrino Oscillations and the Formation of Magma. *Journal of Geoscience and Environment Protection, 12,* 270-287.
https://doi.org/10.4236/gep.2024.1212017

Received: November 20, 2024
Accepted: December 27, 2024
Published: December 30, 2024

Abstract

The current magma formation theory has many shortcomings and is unable to address issues such as the origin of granites and the source of oceanic seamount magmas, and its evolution is ambiguous. Here, based on the latest results of neutrino oscillation-induced radioactive decay research, we analyze the effects of matter in atmospheric neutrino oscillation on the radioactive nuclei in the Earth's interior, as well as the thermal effect caused by this influence, and we propose a new mechanism for the formation of magma. We show that atmospheric neutrinos are able to form a resonance with matter in the Earth as they propagate inside the Earth (i.e., Mikhev-Smirnov-Wolfenstein resonance). This resonance is a collective interaction between atmospheric neutrinos and matter in the Earth, which strongly affects the probability of flavor transitions of atmospheric neutrinos and also influences unstable radioactive nuclei inside the Earth. It stimulates the radioactive nuclei to enter the excited state, increases their decay probability, releases more thermal energy, provides energy for magma formation, extraction, transport, and evolution, and promotes the formation of a low-velocity layer at the lithosphere asthenosphere boundary.

Keywords

Atmospheric Neutrino Oscillations, Effects of Matter, Neutrino Oscillation-Induced Radioactive Decay, Magma Formation, Formation of Asthenosphere

1. Introduction

The formation and evolution of magma is also the formation process of magmatic rocks, which are the main components of the Earth's crust. Clarifying the mechanism of magma formation and evolution is of great significance to understanding of the formation of ancient continents, the formation of new oceanic crust, and the uplift of orogenic belts. Currently, the mainstream magma theory is that magma mainly forms via partial melting of material in the upper mantle and crust. A prerequisite for partial melting of rock to occur is that the temperature must be above its solidus, which can be achieved in two ways: by heating the rock so that it is above the solidus or by lowering the solidus temperature of the rock (e.g., by injecting volatiles or depressurizing the rock) when the temperature is constant. In an environment in which the temperature-pressure gradient is approximately the same everywhere on Earth, if there is no addition of external heat, then the only way to partially melt rocks is to change the temperature-pressure gradient through tectonic movement. Therefore, it is now widely accepted in the geologic community that magma is mainly generated at mid-ocean ridges and in subduction zones. In mid-ocean ridges, the material is depressurized via the upwelling of the deep mantle and asthenospheric material, which contributes to the melting of material (producing magma) (McKenzie and Bickle, 1988). In subduction zones, the material is warmed or volatiles are released from subducted cold slabs into high-temperature horizons, which contributes to the melting of the material (forming magma) (Grove et al., 2012). In addition, experimental petrology research (Bonin and Bébien, 2005; Wu et al., 2007; Wang, 2017) has shown that mantle material cannot form granitic magma directly via partial melting. It can only form basaltic melts, but andesitic melts can also be formed when a large amount of water is present. Basalts can partially form granite via re-melting. Therefore, the upwelling of the asthenosphere cannot form granite directly, and granite can only form through partial re-melting of the oceanic crust caused by subduction. This magma formation theory has many unresolvable problems, such as the origin of granite continents (Bonin and Bébien, 2005; Wu et al., 2007; Wang, 2017; Zhao et al., 2023; Hernández-Uribe, 2024) and seamount magmatism (Machida et al., 2015; Pan et al., 2021). Recent studies have shown that the materials in magma reservoirs may exist mainly in the form of mush, which remains in a less cold fluid storage state for long periods of time, and that the mush in such reservoirs is only activated to generate magmatic activity when new magma intrudes and injects additional heat and fluids (Jackson et al., 2018; Ma et al., 2020). Although this mush model can explain issues such as the tectonic and compositional diversity of granitic bodies, issues such as the source of new magma for mush activation remain unclear.

It is generally believed that the lithospheric mantle and oceanic crust formed in oceanic spreading centers such as mid-ocean ridges correspond to residual bodies and melts (magma), respectively, that have partially melted in the asthenosphere (Xiong, 2021; Xiong et al., 2022). Studies have shown that partial melts were already present in the asthenosphere (Chantel et al., 2016; Debayle et al., 2020), and it was not the upwelling of the asthenosphere that produced these melts. In addition, slab subduction is concentrated in only a few regions, whereas the asthenosphere has a global distribution, so it is unlikely that the melt in the asthenosphere was formed via subduction. That is, the asthenosphere can produce melt without upwelling. At this depth in the asthenosphere, the temperature is only 1000˚C, which is far below the solidus of peridotite (1300˚C), and the heat provided by the ground temperature gradient alone is not enough to cause partial melting of the material in this region. Thus, the mechanism by which partial melting of the material in the asthenosphere occurs remains unclear (Eaton et al., 2009; Chen, 2013; Debayle et al., 2020). In addition, the lithosphere-asthenosphere boundary (LAB) is thought to host a large amount of melt, and there is controversy about the origin of melts in the LAB region (Schmerr, 2012; Naif et al., 2013; Zhang et al., 2024). According to the above summary of previous research, the current theory of magma formation has many flaws and further research is needed to improve it.

Zhang (1999) suggested that the release of heat from solar neutrinos interacting with material in the Earth could lead to the melting of material inside the Earth. However, the cross-section of neutrino interaction with matter is very small, and it is difficult to generate enough energy to cause matter to melt through a general reaction (or absorption). In recent years, some scholars (Jenkins et al., 2009; Sturrock, 2022) have suggested that solar neutrinos may affect the decay rate of radioactive nuclei, but this idea is also controversial (Pommé and Pelczar, 2022). Recently, Zhang and Zhang (2024a) showed that neutrino oscillations are capable of inducing heat generation via radioactive decay. Previous research has focused on the effects of neutrino oscillations on material in the Earth (probability of flavor conversion) (Wolfenstein, 1978; Mikheyev and Smirnov, 1989). To the best of our knowledge, no studies have investigated the effects on nuclei of material in the Earth. The focus of a study conducted by Zhang and Zhang (2024a) was the effect of Mikhev-Smirnov-Wolfenstein (MSW) resonance (Wolfenstein, 1978; Mikheyev and Smirnov, 1989) on unstable radioactive nuclei in matter. It is well known that resonance is a type of forced motion with energetic excitation, which is extremely destructive in fragile systems. MSW resonance, while leading to enhanced neutrino oscillations (i.e., increased probability of flavor transitions), also perturbs the Earth's atoms and excites unstable radionuclides in matter in the Earth, which increases the probability of their decay and releases more heat.

In response to the above problems, in this study, we analyzed the effect of atmospheric neutrino oscillations in the Earth's interior on matter, radiogenic heat generation, and melting of material due to the mechanism of neutrino oscillation-induced radioactive decay (Zhang and Zhang, 2024a). We also investigated and identified a mechanism of magma formation, transport, and evolution and the formation of the asthenosphere. We determined that magma forms mainly in the upper mantle and converges at the LAB under the effect of buoyancy. This magma eventually erupts at mid-ocean ridges to form a new oceanic crust.

2. Method

Based on density data for the Earth's interior provided by the preliminary reference Earth model (PREM) (Dziewonski and Anderson, 1981), the atmospheric neutrino energy spectra provided by Honda et al. (1995) and Gaisser and Honda

(2002), and the element abundances in the Earth's interior provided by Li (1976), we utilized the results of Wolfenstein (1978), Mikheyev and Smirnov (1989) on the theory of MSW resonance on matter, the model of β-decay of atomic nuclei proposed by Fermi (1934), the empirical formula of α-decay constants proposed by Geiger and Nutall (1911), and Zhang and Zhang's (2024a) results on the mechanism of neutrino oscillation-induced radioactive decay and the formation of MSW resonance in the Earth's material when atmospheric neutrinos propagate inside the Earth to investigate the resulting thermal effects.

2.1. Effects of Atmospheric Neutrino Oscillations on Matter

Pontecorvo (1957), Wolfenstein (1978), Mikheyev and Smirnov (1989) investigated the effects of neutrino oscillations on matter and derived a formula for the conversion probability of enhanced neutrino flavors in matter. In the case of a two-flavor neutrino (e.g., $\nu_e \leftrightarrow \nu_\mu$), the conversion probability of the neutrino $\nu_e \to \nu_\mu$ as it propagates through matter with a constant density is

$$P_{\upsilon_e \to \upsilon_\mu} = \sin^2 2\theta_m \sin^2\left(\frac{\Delta m_m^2 L}{4E}\right). \tag{1}$$

The survival rate of the electron neutrino is

$$P_{\upsilon_e \to \upsilon_e} = 1 - \sin^2 2\theta_m \sin^2\left(\frac{\Delta m_m^2 L}{4E}\right). \tag{2}$$

In Equations (1) and (2), E is the energy of the neutrino, L is the length of the oscillation baseline, θ_m is the mixing angle of the effect on matter, and Δm_m^2 is the squared effective mass difference. The correlation between these values is given by the following equations:

$$\tan 2\theta_m = \frac{\Delta m^2 \sin 2\theta}{\Delta m^2 \cos 2\theta - A_{CC}}, \tag{3}$$

$$\Delta m_m^2 = \sqrt{\left(\Delta m^2 \cos 2\theta - A_{CC}\right)^2 + \left(\Delta m^2 \sin 2\theta\right)^2}, \tag{4}$$

where θ is the mixing angle in vacuum, $\Delta m^2 = \left|m_2^2 - m_1^2\right|$ is the squared mass difference between the two mass eigenstates, $A_{CC} \equiv 2EV_{CC} = 2\sqrt{2}EG_F N_e$ is the material potential of the charged matter, G_F is the Fermi constant, and N_e is the number density of the electrons in the matter.

When the following conditions are met, neutrinos will resonate with the atoms in the matter.

$$V\left(N_e\right) = V_{CC} = \sqrt{2}G_F N_e = \frac{\Delta m^2 \cos 2\theta}{2E}. \tag{5}$$

According to the conditions of MSW resonance, in nature, only atmospheric neutrinos (whose energies are 0.1 - 10^4 GeV (Honda et al., 1995; Gaisser and Honda, 2002; Winter, 2016) are able to form resonance with matter in the Earth when they propagate inside the Earth. The energy of an atmospheric neutrino under this resonance is as follows (Winter, 2016):

$$E_{res} = \frac{\Delta m^2 \cos 2\theta}{2\sqrt{2} G_F N_e} \approx \frac{\Delta m_{31}^2 \left[\mathrm{eV}^2\right] \cos 2\theta_{13}}{7.6 \times 10^{-14} \rho \left[\frac{\mathrm{g}}{\mathrm{cm}^3}\right]} \mathrm{eV}. \tag{6}$$

The relationship between N_e and the density of the matter ρ is $N_e = N_A Y_e \rho$, in which N_A is Avogadro's constant, and Y_e is the electron fraction. MSW resonance can be formed when the atmospheric neutrino energy E_{res} and the density of matter in ρ satisfy Equation (6).

2.2. Neutrino Potential of Matter in the Earth

When neutrinos oscillate, the weak interaction field formed by the neutrinos reacts against the atoms in the matter. Based on the effective potential of matter acting on neutrinos (i.e., the matter potential of neutrinos), the effective potential of electron neutrinos acting on matter, i.e., the (charge-flow) neutrino potential felt by the matter, can be obtained:

$$V\left(N_{\upsilon_e}\right) = \sqrt{2} G_F N_{\upsilon_e}, \tag{7}$$

where N_{υ_e} is the number density of the neutrinos. Assuming that the electron neutrino flux is constant and has magnitude $\varnothing_0$, the electron neutrino flux after propagating a distance of L is

$$\varnothing_L = \varnothing_0 P_{\upsilon_e \to \upsilon_e} = \varnothing_0 \left[1 - \sin^2 2\theta_m \sin^2\left(\frac{\Delta m_m^2 L}{4E}\right)\right]. \tag{8}$$

Since the speed of the neutrino is close to the speed of light c, the distance traveled by the electron neutrino per unit time is c, and the number density of the electron neutrinos is

$$N_{\upsilon_e} = \frac{\varnothing_L}{c} = \frac{\varnothing_0 P_{\upsilon_e \to \upsilon_e}}{c} = \frac{\varnothing_0}{c}\left[1 - \sin^2 2\theta_m \sin^2\left(\frac{\Delta m_m^2 L}{4E}\right)\right]. \tag{9}$$

Substituting Equation (9) into Equation (7) yields

$$V\left(N_{\upsilon_e}\right) = \frac{\sqrt{2} G_F \varnothing_0}{c}\left[1 - \sin^2 2\theta_m \sin^2\left(\frac{\Delta m_m^2 L}{4E}\right)\right]. \tag{10}$$

At resonance, $\theta_m \to \pi/4$, and Equation (10) can be simplified to

$$V\left(N_{\upsilon_e}\right) = \frac{\sqrt{2} G_F \varnothing_0}{c}\left[1 - \sin^2\left(\frac{\Delta m_m^2 L}{4E}\right)\right] = \frac{\sqrt{2} G_F \varnothing_0}{c} \cos^2\left(\frac{\Delta m_m^2 L}{4E}\right). \tag{11}$$

Equation (11) is the neutrino potential of the electron neutrino action on the atoms of the matter in the resonance region. This effective potential is weak, but since the resonance is capable of accumulating energy, the necessary excitation energy can eventually be obtained.

2.3. Theory of Radioactive Decay

Fermi (1934) derived an expression for the decay constant for the beta decay of atomic nuclei:

$$\lambda = \int_0^{P_m} \frac{g^2 \left|M_{if}\right|^2}{2\pi^3 c^3 \hbar^7} F\left(Z,R,P\right) P^2 \left(E_m - E\right)^2 \mathrm{d}P, \tag{12}$$

where g is the weak interaction coupling constant, P and E are the momentum and energy of the radiating electrons, respectively, and P_m and E_m are the maximum electron momentum and maximum electron energy of the radiating electrons, respectively. $F\left(Z,R,P\right)$ is the Coulomb correction factor, which describes the effect of the Coulomb field of the nucleus on the emitted β-particles, and is a function of the subnucleus charge Z, radius R, and energy of the β-particle E. $\left|M_{if}\right|$ is the leapfrog matrix element associated with the subnucleus and the parent nucleus. The magnitude of the lepton probability is mainly determined by the magnitude of the lepton matrix elements $\left|M_{if}\right|$.

When $E_m \gg m_e c^2$ and $F\left(Z,E\right) \approx 1$, $F\left(Z,E_m\right) = AE_m^5$ (where A is a constant),

$$\lambda \propto E_m^5 . \tag{13}$$

Geiger and Nutall (1911) derived the following empirical formula for the alpha decay constant:

$$\lambda \propto E_\alpha^{86.25}, \tag{14}$$

where E_α is the kinetic energy of the α particle.

2.4. Calculation of Radioactive Heat Generation

Studies have shown that melts in the Earth's interior are mainly distributed in the upper mantle (Debayle et al., 2020). The most dominant radioisotopes in the upper mantle are ^{238}U, ^{232}Th, and ^{40}K, which have contents of about 0.13 × 10^{-6}, 0.75 × 10^{-6}, and 0.23% × 0.0117%, respectively (Li, 1976). The decay reaction equations of which are as follows (Fiorentini et al., 2007):

$$^{238}\mathrm{U} \rightarrow {}^{206}\mathrm{Pb} + 8\alpha + 6\mathrm{e}^- + 6\overline{\nu}_e + 51.7\ \mathrm{MeV}, \tag{15}$$

$$^{232}\mathrm{Th} \rightarrow {}^{208}\mathrm{Pb} + 6\alpha + 4\mathrm{e}^- + 4\overline{\nu}_e + 42.7\ \mathrm{MeV}, \tag{16}$$

$$^{40}\mathrm{K} \rightarrow {}^{40}\mathrm{Ca} + \mathrm{e}^- + \overline{\nu}_e + 1.31\ \mathrm{MeV}. \tag{17}$$

The energy released by the decay of radioactive elements can be calculated as follows:

$$E = N_A \frac{M}{g} Q, \tag{18}$$

where M is the mass of the radioactive element, g is its molar molecular weight, $N_A = 6.022 \times 10^{23}\ \mathrm{mol}^{-1}$ is Avergadro's constant, and Q is the energy released by the decay of a radioactive atom.

Assuming that in the upper mantle, there is a layer of material with a thickness of dr, that all of the energy $\mathrm{d}\Omega$ released by the radioactive material is used for heating and melting the material in this layer, that the heat consumed by the mantle for heating during this process is $\mathrm{d}\Omega'$, that the heat consumed for melting, i.e., the latent heat of fusion, is $\mathrm{d}\Lambda$,

$$d\Omega = d\Omega' + d\Lambda. \tag{19}$$

In this small region, the pressure and temperature are almost constant, so Equation (19) can be approximated as

$$\Omega = \Omega' + \Lambda. \tag{20}$$

For example, if this small region of upper mantle material has a mass of 1000 kg, Equation (20) can be used to calculate the total heat required to melt the material: $\Omega = \Omega' + \Lambda = 5.1\times10^8$ J. For 1000 kg of the upper mantle material in the main radioactive substances, the total decay-produced heat of up to 1.69×10^{10} J is much higher than the amount required to completely melt the upper mantle material.

In the above calculations, the constant-pressure specific heat capacity of the rocks is taken to be 1000 J/(kg·K) (Shui and Watanabe, 1982; Zhang, 2001; Chen, 2013). The average temperature of the upper mantle is taken to be 1000˚C (or 1273 K), the melting temperature of the material at the same depth is taken to be 1300˚C (or 1573 K), and the latent heat of fusion of the upper mantle is taken to be 210 kJ/kg (Shui and Watanabe, 1982).

2.5. Limitations of the Proposed Method

The origin of the effect of neutrino oscillations on matter is caused by forward coherent scattering between the neutrinos and matter. Although this coherent scattering is capable of delivering a weak momentum (or energy) to matter (Freedman, 1974; Akimov et al., 2017), we were unable to obtain the exact energy delivered to the radioactive nuclei by the neutrino oscillations (MSW resonances) through theoretical calculations. Thus, the estimation of the radioactive decay rate is very rough. Therefore, it is necessary to obtain the real value of the change in the decay rate caused by neutrino oscillation-induced radioactive decay, and experimental probes are needed to determine it. In this study, we established the simplest experimental method. Considering that the density of the water body is the most homogeneous and it is easy for MSW resonance to occur, several samples of a certain radioisotope can be placed in the range of 2.0 - 7.0 km in the ocean depth, and the change in the decay rate with respect to that at the surface can be obtained to determine the required value. This can also be used to test the theory developed in this study.

3. Results and Discussion

The density of the Earth varies within a range of approximately 1 - 13 g/cm^3 from the oceans to the Earth's core (Dziewonski and Anderson, 1981). According to the conditions under which neutrino oscillations generate MSW resonance (Wolfenstein, 1978; Mikheyev and Smirnov, 1989), the energy at which neutrinos form resonance within the Earth's interior can be calculated to be 2.42 - 31.5 GeV, indicating that only atmospheric neutrinos are able to form broad MSW resonances as they propagate through the interior of the Earth. The excitation energy of this resonance is the weak charge-flow effective potential. Considering that the average energy (or energy flow) of atmospheric neutrinos resonating in the mantle region is about 10 GeV (Honda et al., 1995; Gaisser and Honda, 2002) and that the maximum excitation energy produced by their couplings with matter is ~10^5 eV, it can be assumed that the excitation energy of this resonance is all obtained by the α-particles. Moreover, according to the empirical equation for the α-decay constant proposed by Geiger and Nutall (1911), the change in the decay rate of the α-decay under the resonant excitation of neutrino oscillations can be estimated. For example, the energy of the alpha particle produced by the decay of $^{238}_{92}U$ is 4.2 MeV, and the effective potential of the atmospheric neutrino affecting the matter is $V\left(N_{\upsilon_e}\right)=\frac{\sqrt{2}G_F\varnothing_0}{c}\cos^2\left(\frac{\Delta m_m^2 L}{4E}\right)$, where $\frac{\varnothing_0}{c}\sim 10$ GeV is the atmospheric neutrino flux, so the maximum value of $V\left(N_{\upsilon_e}\right)$ is about ~10^5 eV. If the atmospheric neutrino is able to use all of its effective potential for the excitation of $^{238}_{92}U$ when it is in resonance with the matter and all of the excitation energy is converted into the kinetic energy of the α-particle, then its decay constant or decay rate would increase by a factor of 7.6. Although this estimate is not rigorous (because the maximum effective potential cannot be fully converted into the excitation energy of the resonance and the flux of atmospheric neutrinos cannot be calculated precisely), it is entirely possible for the radioactive nuclei to accumulate ~10^5 eV or even more through resonance since the resonance energy can be accumulated. Therefore, this calculation is still informative.

Our calculations show that in the upper mantle, as little as 3.02% of the radioactive elements are promoted to decay by the MSW effect, and the heat generated is sufficient to cause the material in this region to melt.

3.1. Effects of Neutrino Oscillations on α-Decay

Zhang and Zhang (2024a) have shown that although the MSW effect of neutrino oscillations is a weak interaction resonance, it can also have an effect on alpha decay. The reason for this is that in neutrino oscillations, there are some couplings and connections between the weak interactions and the strong interactions (Higgs, 1964, 2014; Weinberg, 1967), which are able to induce oscillations in the Higgs field and thus excite α decay. Indeed, as a result of this weak interaction, the weak effective potential is converted into energy when the MSW resonance is generated. This energy is transferred to the atoms in the entire medium involved in the resonance in the form of resonance, which transitions the atoms in an excited state (**Figure 1**), and since α-decay is very sensitive to energy, MSW resonance is able to increase the probability of α-decay.

3.2. Formation, Extraction, Transport, and Evolution of Magma

A melt pocket is a micro-melting zone originating from the mantle. Its size is in the nanometer to micrometer range, and it is considered the beginning or basic unit of magma. A melt pocket usually consists of neonate minerals + molten glass + residual minerals after melting (**Figure 2**). It has various shapes, including

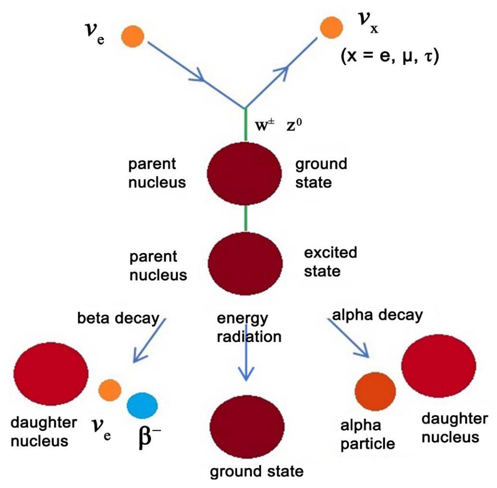

Figure 1. Neutrino oscillations perturb radioactive nuclei to decay in an excited state.

droplet, spherical, fan, cowl, vein, and indeterminate shapes (Liu, 2020). The development of melt pocket is found all over the globe and has been studied by many scholars (Du, 1998; Su et al., 2010; Liu, 2020). It has been found that in the same rock section of the same orthorhombic pyroxene (Opx), some particles are completely melted, while others are not melted, and the degree of melting varies greatly within a thin layer, indicating that they are not in the same thermal field (Du, 1998). In addition, the prevalence of glassiness in the micromelting zone (Liu, 2020) indicates that the melt pocket underwent rapid cooling after melting and that there is a large temperature difference between the melt pocket and the surrounding environment. Obviously, this melt pocket could not have been produced via plate subduction or mantle upwelling, and it should have a different origin. According to Du (1998), the uneven infiltration of mantle fluids leading to the melting of material is an important factor in the formation of magma (a melt pocket). However, the melt pocket is not connected to the surrounding material by fissures or magma veins, and the flow of mantle material (including gases) cannot penetrate into the melt pocket.

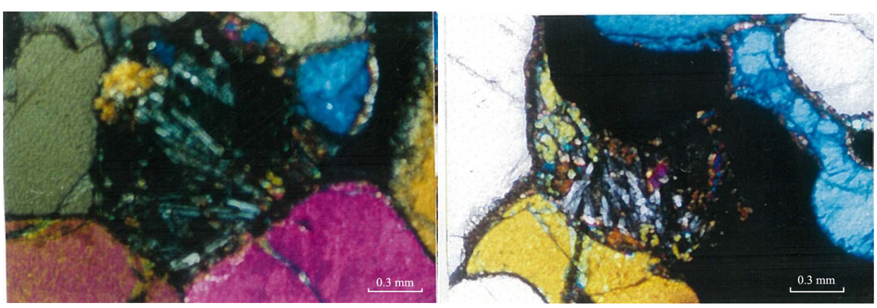

(a) (b)

Figure 2. Jiaohe melt pocket. (a) Melt pocket 1 occurs between olivine and orthopyroxene crystals. Its diameter is about 2.5 mm. (b) Melt pocket 2 occurs in the gaps between orthopyroxene and spinel crystals. It has an ox-horn shape and the particle size is 1.5 - 2.0 mm. The images are from Liu (2020).

We believe that the only factor that can cause the melt to penetrate deep into the minerals without destroying them and cause melting in the microzones in the middle of the minerals is atmospheric neutrinos. Since neutrino oscillations can only induce radioactive decay, melting can only occur in areas enriched in radioactive elements, and the first material to melt is the area enriched in radioactive elements. A melt pocket consists of typical radioactive element-enriched microregions. Du and Wang (2005) showed that in the mantle, radioactive U is the least abundant in mineral crystals, in which it does not exceeding 10×10^{-9}, and it is more abundant in crystal boundaries and cleavage planes (generally tens to hundreds of 10^{-9}). The melt pocket is the most uranium-enriched material. For example, the uranium mass fraction of the melt pocket of sample JH4 is (323.85 - 1125.1) 10^{-9}. In addition, the melt pocket is unusually enriched in K (Du, 1998; Liu, 2020), and ^{40}K is also the major radioisotope in the Earth's interior. This is a strong indication that melting is closely related to the enrichment of radioactive elements. When atmospheric neutrinos propagate through the mantle and generate MSW resonance, the regions enriched in radioactive elements are strongly heated, causing the material to melt. At this time, the temperature of the molten microregion is significantly higher than the ambient temperature. When atmospheric neutrinos stop passing through the melting microregion due to certain effects (such as interference from geomagnetic storms), the decay of the radioactive elements returns to its natural state, the heat generation is suddenly reduced, and the temperature of the melting region drops rapidly. As a result, some of the molten material will crystallize into minerals due to the drop in temperature, and some of the molten material will solidify into glassy material before it can be crystallized. If atmospheric neutrinos propagate through the solidified micro-area (melt pocket) again, the micro-area will melt again, and new minerals will crystalize. This is the fundamental reason for the diversity and complexity of the new minerals and their combinations in molten microzones (Du, 1998; Liu, 2020).

The distribution of the radioisotopes in the mantle is heterogeneous (Dai et al., 2005; Wu et al., 2021). The regions where the radioactivity is perturbed by neutrino oscillations, which generate heat and cause melting, are consequently inhomogeneous, with melting occurring only in the small regions that are relatively enriched in radioactive elements, forming a series of melt pockets (Liu, 2020). As the heat generated by the radioactive elements via perturbation caused by neutrino oscillations increases and the temperature increases, the melt pocket grows gradually, or the melt pockets grow and then converge together to form a larger melt. When the proportion of melt reaches 0.02% - 0.20%, the melt is interconnected between mineral particles, and due to the high temperature and low density of the melt, a large buoyancy force is generated and the melt can be easily extracted from the minerals and transported upward due to this buoyancy force (Zhu et al., 2011; Sawyer et al., 2011).

Due to the good peristaltic properties of the mantle, melts migrate and converge along the edges of particles in a permeable manner in the mantle. When melt penetrates along the edge channels of particles, there is a power law relationship between the melt ratio and the permeability (Wark and Watson, 1998; Bons et al., 2004). Therefore, as the amount of melt increases slightly, the permeability significantly increases. When the local mantle melt ascends, migrates, and converges with rock layers with poor peristalsis and rigid crust, it is usually difficult for the melt to ascend and migrate in a permeable manner, and it can only migrate along cracks or faults, can form magma chambers or mush in suitable areas, or can reactivate previously formed cold mush (Jackson et al., 2018; Ma et al., 2020).

The process of the ascent of the magma is also the process of continuous evolution of the magma. In this process, the magma continuously exchanges material and energy with the surrounding environment through merging, fusion, accumulation, alteration, crystallization, and dissolution, which ultimately leads to the continuous melting of fusible materials along the magma's path (clearing of the path), while refractory materials continue to crystallize and accumulate, and some of the structures in the deep part of the Earth also constantly change (**Figure 3**).

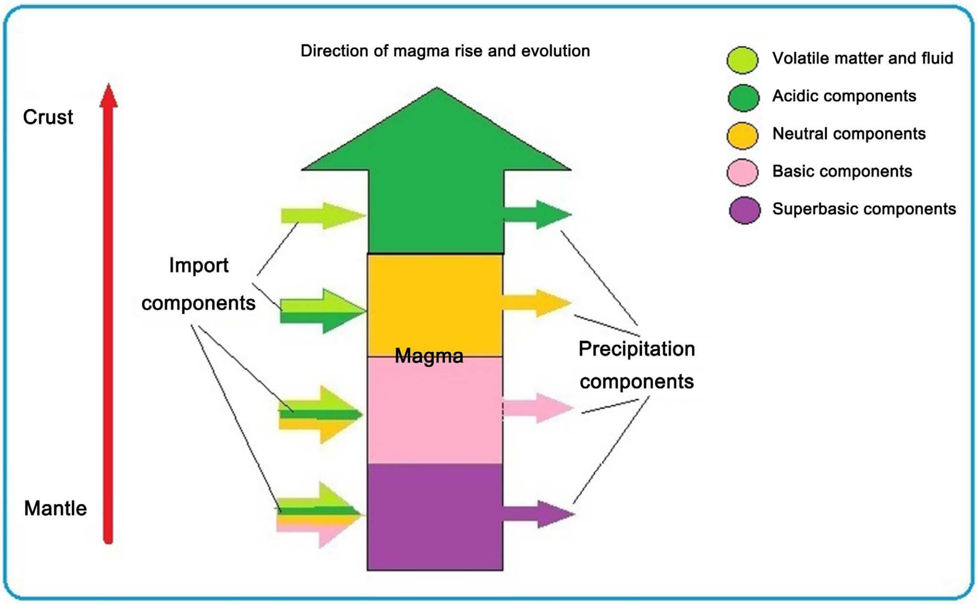

Figure 3. Schematic diagram showing the depth variations of the molten components added and the mineral components precipitated during magma ascent and evolution.

In addition, from the formation and evolution of the magma, it can also be concluded that the process of magma formation is actually the extraction of fusible materials and elements such as radioisotopes from the upper mantle and asthenosphere, as well as the continuous sorting out of materials in the lower crust (possibly including the middle crust) (Takazawa et al., 1992). After a long geologic time period, the result of these processes is the formation of refractory ultramafic rocks with losses of corresponding elements in the upper mantle, basaltic rocks (coexisting with residues and precipitates) in the lower crust, and evolutionarily mature silicic rocks enriched in the relevant elements in the upper crust.

3.3. Distribution of Mantle Melts and Genesis of the Asthenosphere and LAB

Calculations have shown that atmospheric neutrinos are able to form MSW resonance with matter in all of the layers of the Earth, and accordingly melts should be widely distributed in all of the layers of the Earth. However, geophysical surveys indicate that melts are mainly concentrated in the upper mantle and the asthenosphere (**Figure 4**) (Debayle et al., 2020). This may be due to a number of reasons. 1) Since there is a resonance initiation process, it is difficult to produce MSW effects in the shallow crust, and therefore the radioactive materials in the crust are not perturbed by MSW resonance to generate heat. Thus, there is usually no molten material in the crust. 2) Since the upper mantle has a greater concentration of radioactive elements, the radioactive decay due to MSW resonance is able to generate enough heat to cause some of the material to melt. By contrast, the lower mantle has a lower concentration of radioactive elements, and coupled with the increased pressure, the radioactive heat generation promoted by the MSW effect is not sufficient to cause the material to melt. The aforementioned calculations reveal that in the upper mantle, the situation in which 3.02% of the radioactive elements are induced to decay by the MSW effect is sufficient to lead to melting of the material. In the lower mantle, the contents of radioactive elements ^{238}U, ^{232}Th, and ^{40}K are about 0.003×10^{-6}, 0.005×10^{-6}, $0.03\% \times 0.0117\%$, respectively (Li, 1976). Using these data, it can be calculated that the heat of decay of all of the radioactive material contained in 1000 kg of lower mantle material is only 2.62×10^8 J. This heat is less than the heat required to melt 1000 kg of upper mantle material (i.e., 5.1×10^8 J). Because the pressure in the lower mantle is high relative to that in the upper mantle, melting the same amount of material requires more heat, so it is difficult for the heat produced via decay of the radioactive elements in the lower mantle to completely melt the lower mantle material. 3) Atmospheric neutrino oscillations and the radioactive decay they promote are both probabilistic events, and such probabilistic events are generally normally distributed. That is, from the spatial perspective, a more concentrated region of heat generation and melting exists, and the amounts of heat generation and melting gradually decrease upward and downward with this region as a base point. This region of melt concentration is the asthenosphere. 4) The uneven distribution of atmospheric neutrinos is generated via cosmic ray perturbations by the geomagnetic field, and therefore the radioactive heat generation promoted by their oscillations exhibits an uneven distribution. This can result in an uneven distribution of melt in the lateral direction. 5) Due to the arch tectonic effect (Zhang and Zhang, 2024b), melt beneath the basins (flats) on either side of the range converges toward the range, resulting in more melt beneath the range. 6) There may also be other unknown influencing factors.

Once the melt is produced in the upper mantle and the asthenosphere, it ascends and converges under the effect of buoyancy. As the height of the ascent increases, the temperature of the melt decreases, the viscosity increases, and the creep of the mantle decreases. Thus, when the melt arrives in the upper mantle lithosphere, due to the permeability barrier at the lower boundary of the lithosphere, it is difficult for the magma to ascend by means of permeability, and it can only be transported upward along fissures and fractures. As a result, a large amount of melt is trapped at the LAB, leading to a large increase in the melt content in this region and thus forming a sharp seismic wave discontinuity interface (Schmerr, 2012; Zhang et al., 2024). Since the melt in the asthenosphere is the product of in situ melting, the melt is more silicon-poor and iron-rich, and the melt that converges in the LAB is usually considered asthenospheric melt that has ascended to the base of the lithosphere along grain boundaries (Schmerr, 2012). This melt crystallizes and precipitates some of the ultramafic minerals due to the occurrence of heat dissipation during the migration process, resulting in the occurrence of a relatively silicon-rich and iron-poor melt in this area (Zhang et al., 2024).

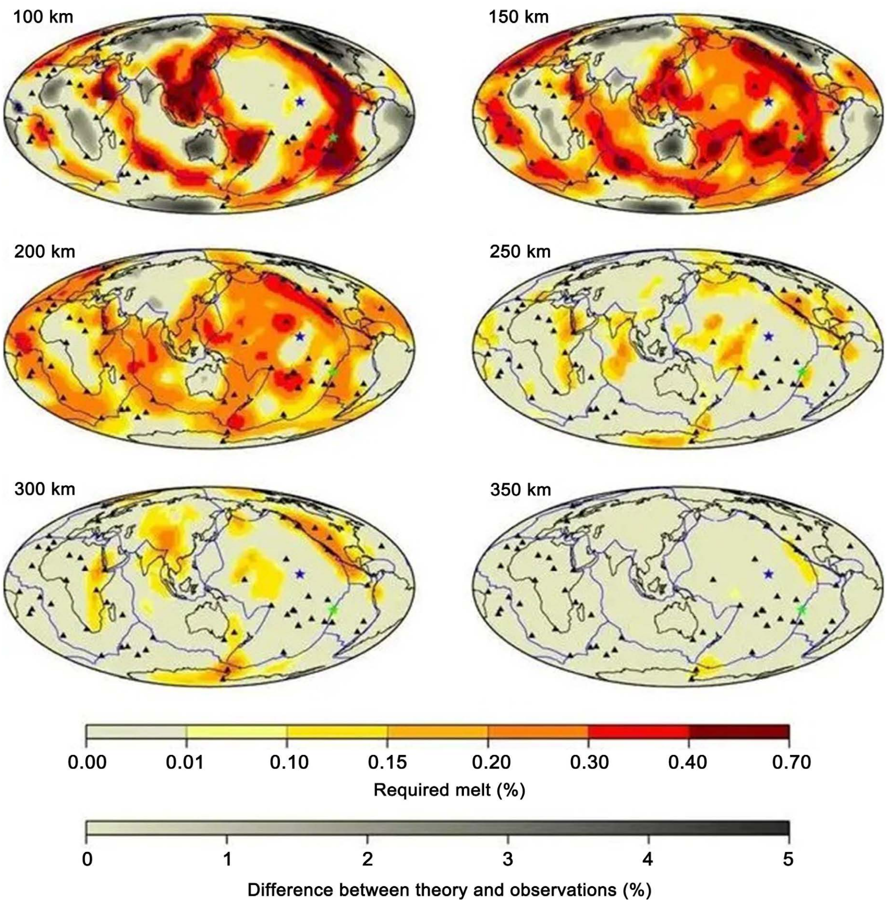

Figure 4. Melt contents at different depths in the upper mantle. The images are from Debayle et al. (2020).

3.4. Mechanisms of the Formation of New Oceanic Crust at Mid-Ocean Ridges

As the convergence of high-temperature melts at the LAB increases, the lithosphere gradually thins via melt erosion (Hyndman and Canil, 2021; Sato & Ozawa, 2023). The lithosphere is also subjected to increasing thermal pressure, which ultimately leads to uplift and tearing of the thinner and reduction of the compressive strength of the oceanic lithosphere. As a result, the melt that was trapped at the LAB ascends along the fractures and eventually erupts onto the ocean floor, forming a new oceanic crust. When the thermal pressure is released and the melt (magma) is not replenished, the magma stops erupting. The damaged oceanic crust is then filled with the magma, and when the magma is completely solidified, the lithospheric and oceanic crust are repaired, and the gravitational force exerted by the overlying rocks and the thermal pressure are balanced again. However, the radioactive decay induced by atmospheric neutrino oscillations does not stop, and magma is still gradually generating and ascending, converging toward the LAB. When the thermal pressure exerted by the converging magma is greater than the gravitational force exerted by the overlying rocks, once again the lithosphere and oceanic crust are damaged and fractured, the magma once again erupts along the fractures, the thermal pressure is released, new oceanic crust is formed, and the lithosphere and the oceanic crust are repaired. As a result, the height of the mid-ocean ridge increases, and movement of the oceanic lithosphere and oceanic crust is promoted. Of course, if there are weak structures such as cracks and fractures within the oceanic plate, the melt present under the lithosphere can also ascend and erupt along the cracks and fractures, forming a number of seamounts of varying sizes on the seafloor (Machida et al., 2015; Pan et al., 2021).

4. Conclusion

The MSW resonance on matter can accelerate the decay of unstable radioactive elements in the Earth's interior, generating heat and leading to melting of the material in regions enriched in radioactive elements. Since the upper mantle is enriched in radioactive elements, the heat released from their radioactive decay induced by MSW resonance can lead to partial melting of the material in this region and the formation of the asthenosphere. Initially, the melt generated is randomly distributed in the upper mantle. As a result of the high temperature, low density, and low viscosity of the melt, it slowly ascends, converges, and is transported along mineral interstices via osmosis under the action of a large buoyancy force. When the melt reaches the poorly peristaltic lithosphere, it cannot continue to ascend via osmosis, and it can only ascend and be transported along fractures and fissures. Thus, much of the melt is stagnant and converges at the LAB. The melt convergence at the LAB increases and great thermal pressure is generated and exerted on the overlying lithosphere. When this thermal pressure increases to a certain level, it causes the crust in the weakest region of the lithosphere (mid-ocean ridges) to rupture, and the melt along the cracks erupts, cools, and solidifies on the ocean floor to form new oceanic crust. When ocean basins are fractured by tectonic movements, magma also erupts along these fractures and forms seamounts.

The above conclusion is only a qualitative description, and this paper has not been able to give quantitative calculation results. Since the energy transported by resonance is difficult to measure and can be accumulated, it is difficult to calculate and determine the specific excitation energy obtained by a radioactive nucleus, and thus the decay rate and heat generation of a neutrino-induced radioactive nucleus cannot be calculated. These values can be determined by further experimental investigations.

Background Explanation and Acknowledgements

The main content of this paper was presented orally at the 22nd National Symposium on Mineral Inclusions and Geological Fluids, China 2024, and an abstract was submitted under the title "Atmospheric Neutrino Oscillations and the Origin of Magmatic and Mantle Fluids". We thank the scholars who participated in discussions on this topic and encouraged the authors during the conference.

Conflicts of Interest

The authors declare no conflicts of interest regarding the publication of this paper.

References

Akimov, D., Albert, J. B., An, P., Awe, C., Barbeau, P. S., Becker, B. et al. (2017). Observation of Coherent Elastic Neutrino-Nucleus Scattering. *Science, 357,* 1123-1126. https://doi.org/10.1126/science.aao0990

Bonin, B., & Bébien, J. (2005). The Granite-Upper Mantle Connection in Terrestrial Planetary Bodies: An Anomaly to the Current Granite Paradigm? *Lithos, 80,* 131-145. https://doi.org/10.1016/j.lithos.2004.03.059

Bons, P. D., Arnold, J., Elburg, M. A., Kalda, J., Soesoo, A., & van Milligen, B. P. (2004). Melt Extraction and Accumulation from Partially Molten Rocks. *Lithos, 78,* 25-42. https://doi.org/10.1016/j.lithos.2004.04.041

Chantel, J., Manthilake, G., Andrault, D., Novella, D., Yu, T., & Wang, Y. (2016). Experimental Evidence Supports Mantle Partial Melting in the Asthenosphere. *Science Advances, 2,* e1600246. https://doi.org/10.1126/sciadv.1600246

Chen, Z. G. (2013). The Earth Expansion Generated the Asthenosphere and Its Formation Time. *Advance in Earth Sciences, 28,* 834-846. https://doi.org/10.11867/j.issn.1001-8166.2013.07.0834

Dai, T. G., Gong, L. L., & Zhang, Q. Z. (2005). *Applied Geochemistry Changsha*. Central South University Press.

Debayle, E., Bodin, T., Durand, S., & Ricard, Y. (2020). Seismic Evidence for Partial Melt Below Tectonic Plates. *Nature, 586,* 555-559. https://doi.org/10.1038/s41586-020-2809-4

Du, L. T., & Wang, W. G. (2005). Occurrence States of Uranium in the Mantle and Their Geo-Chemical Implication. *Earth Science Frontiers, 12,* 69-78. https://doi.org/10.3321/j.issn:1005-2321.2005.01.011

Du, L. T. (1998). Mantle Fluids and Magma Origin of Basalts and Alkaline Rocks. *Earth Science Frontiers, 5,* 145-157.

Dziewonski, A. M., & Anderson, D. L. (1981). Preliminary Reference Earth Model. *Physics of the Earth and Planetary Interiors, 25,* 297-356. https://doi.org/10.1016/0031-9201(81)90046-7

Eaton, D. W., Darbyshire, F., Evans, R. L., Grütter, H., Jones, A. G., & Yuan, X. (2009). The Elusive Lithosphere-Asthenosphere Boundary (LAB) beneath Cratons. *Lithos, 109,* 1-22. https://doi.org/10.1016/j.lithos.2008.05.009

Fermi, E. (1934). Versuch einer Theorie der β-Strahlen. I. *Zeitschrift für Physik, 88,* 161-177. https://doi.org/10.1007/bf01351864

Fiorentini, G., Lissia, M., & Mantovani, F. (2007). Geo-Neutrinos and Earth's Interior. *Physics Reports, 453,* 117-172. https://doi.org/10.1016/j.physrep.2007.09.001

Freedman, D. Z. (1974). Coherent Effects of a Weak Neutral Current. *Physical Review D, 9,* 1389-1392. https://doi.org/10.1103/physrevd.9.1389

Gaisser, T. K., & Honda, M. (2002). Flux of Atmospheric Neutrinos. *Annual Review of Nuclear and Particle Science, 52,* 153-199. https://doi.org/10.1146/annurev.nucl.52.050102.090645

Geiger, H., & Nuttall, J. M. (1911). LVII. *The Ranges of the A Particles from Various Radioactive Substances and a Relation between Range and Period of Transformation. The London, Edinburgh, and Dublin Philosophical Magazine and Journal of Science, 22,* 613-621. https://doi.org/10.1080/14786441008637156

Grove, T. L., Till, C. B., & Krawczynski, M. J. (2012). The Role of H_2O in Subduction Zone Magmatism. *Annual Review of Earth and Planetary Sciences, 40,* 413-439. https://doi.org/10.1146/annurev-earth-042711-105310

Hernández-Uribe, D. (2024). Generation of Archaean Oxidizing and Wet Magmas from Mafic Crustal Overthickening. *Nature Geoscience, 17,* 809-813. https://doi.org/10.1038/s41561-024-01489-z

Higgs, P. W. (1964). Broken Symmetries, Massless Particles and Gauge Fields. *Physics Letters, 12,* 132-133. https://doi.org/10.1016/0031-9163(64)91136-9

Higgs, P. W. (2014). Nobel Lecture: Evading the Goldstone Theorem. *Reviews of Modern Physics, 86,* 851-853. https://doi.org/10.1103/revmodphys.86.851

Honda, M., Kajita, T., Kasahara, K., & Midorikawa, S. (1995). Calculation of the Flux of Atmospheric Neutrinos. *Physical Review D, 52,* 4985-5005. https://doi.org/10.1103/physrevd.52.4985

Hyndman, R. D., & Canil, D. (2021). Geophysical and Geochemical Constraints on Neogene-recent Volcanism in the North American Cordillera. *Geochemistry, Geophysics, Geosystems, 22,* GC009637. https://doi.org/10.1029/2021gc009637

Jackson, M. D., Blundy, J., & Sparks, R. S. J. (2018). Chemical Differentiation, Cold Storage and Remobilization of Magma in the Earth's Crust. *Nature, 564,* 405-409. https://doi.org/10.1038/s41586-018-0746-2

Jenkins, J. H., Fischbach, E., Buncher, J. B., Gruenwald, J. T., Krause, D. E., & Mattes, J. J. (2009). Evidence of Correlations between Nuclear Decay Rates and Earth-Sun Distance. *Astroparticle Physics, 32,* 42-46. https://doi.org/10.1016/j.astropartphys.2009.05.004

Li, T. (1976). Chemical Element Abundances in the Earth and Its Major Shells. *Geochimica, 5,* 167-174. https://doi.org/10.19700/j.0379-1726.1976.03.001

Liu, J. H. (2020). Mineralogy and Geological Significance of the Melting Zone in the Jiaohe Upper Mantle Fragment, Jilin. *Earth Science Frontiers, 27,* 48-60. https://doi.org/10.13745/j.esf.sf.2020.5.50

Ma, C. Q., Zou, B. W., Gao, K., Wen, X. (2020). Crystal Mush Storage, Incremental Pluton Assembly and Granitic Petrogenesis. *Earth Science, 45,* 4332-4351.

Machida, S., Hirano, N., Sumino, H., Hirata, T., Yoneda, S., & Kato, Y. (2015). Petit-spot Geology Reveals Melts in Upper-Most Asthenosphere Dragged by Lithosphere. *Earth and Planetary Science Letters, 426,* 267-279. https://doi.org/10.1016/j.epsl.2015.06.018

McKenzie, D., & Bickle, M. J. (1988). The Volume and Composition of Melt Generated by Extension of the Lithosphere. *Journal of Petrology, 29,* 625-679. https://doi.org/10.1093/petrology/29.3.625

Mikheyev, S. P., & Smirnov, A. Y. (1989). Resonant Neutrino Oscillations in Matter. *Progress in Particle and Nuclear Physics, 23,* 41-136. https://doi.org/10.1016/0146-6410(89)90008-2

Naif, S., Key, K., Constable, S., & Evans, R. L. (2013). Melt-Rich Channel Observed at the Lithosphere-Asthenosphere Boundary. *Nature, 495,* 356-359. https://doi.org/10.1038/nature11939

Pan, M. H., Yang, T., Lin J., Zhang, F., Zhou, Z. Y., Li, H. Y. et al. (2021). The Formation Mechanism of Petit-Spot Volcanoes and the Nature of the Lithosphere-Asthenosphere Boundary (LAB). *Earth Science, 46,* 817-825. https://doi.org/10.3799/dqkx.2020.340

Pommé, S., & Pelczar, K. (2022). Neutrino-Induced Decay: A Critical Review of the Arguments. *Space Science Reviews, 218,* Article No. 64. https://doi.org/10.1007/s11214-022-00932-0

Pontecorvo, B. (1957). Mesonium and Anti-Mesonium. *Sovietic Journal of Experimental and Theoretical Physics, 33,* 549-551.

Sato, Y., & Ozawa, K. (2023). Thermal Evolution of the Lithosphere-Asthenosphere Boundary beneath Arc and Its Geodynamic Implications: Depth Variation of Thermal Histories of Mantle Xenoliths from Ichinomegata, Northeast Japan. *Journal of Geophysical Research: Solid Earth, 128,* JB027208. https://doi.org/10.1029/2023jb027208

Sawyer, E. W., Cesare, B., & Brown, M. (2011). When the Continental Crust Melts. *Elements, 7,* 229-234. https://doi.org/10.2113/gselements.7.4.229

Schmerr, N. (2012). The Gutenberg Discontinuity: Melt at the Lithosphere-Asthenosphere Boundary. *Science, 335,* 1480-1483. https://doi.org/10.1126/science.1215433

Shui, G. R., & Watanabe, H. (1982). The Earth's Thermology, Yan Bo Lecture, Earth Science. In *Research on the Basic Theory of Geothermal* (p. 35). Geological Publishing House.

Sturrock, P. A. (2022). Neutrino-Flux Variability, Nuclear-Decay Variability, and Their Apparent Relationship. *Space Science Reviews, 218,* Article No. 23. https://doi.org/10.1007/s11214-022-00878-3

Su, B., Zhang, H., Sakyi, P. A., Qin, K., Liu, P., Ying, J. et al. (2010). Formation of Melt Pocket in Mantle Peridotite Xenolith from Western Qinling, Central China: Partial Melting and Metasomatism. *Journal of Earth Science, 21,* 641-668. https://doi.org/10.1007/s12583-010-0116-y

Takazawa, E., Frey, F. A., Shimizu, N., Obata, M., & Bodinier, J. L. (1992). Geochemical Evidence for Melt Migration and Reaction in the Upper Mantle. *Nature, 359,* 55-58. https://doi.org/10.1038/359055a0

Wang, X. L. (2017). Some New Research Progresses and Main Scientific Problems of Granitic Rocks. *Acta Petrologica Sinica, 33,* 1445-1458. http://www.ysxb.ac.cn/article/id/5ff2dd20bfedb51e1a6ae428

Wark, D. A., & Watson, E. B. (1998). Grain-Scale Permeabilities of Texturally Equilibrated, Monomineralic Rocks. *Earth and Planetary Science Letters, 164,* 591-605. https://doi.org/10.1016/s0012-821x(98)00252-0

Weinberg, S. (1967). A Model of Leptons. *Physical Review Letters, 19,* 1264-1266. https://doi.org/10.1103/physrevlett.19.1264

Winter, W. (2016). Atmospheric Neutrino Oscillations for Earth Tomography. *Nuclear Physics B, 908,* 250-267. https://doi.org/10.1016/j.nuclphysb.2016.03.033

Wolfenstein, L. (1978). Neutrino Oscillations in Matter. *Physical Review D, 17,* 2369-2374. https://doi.org/10.1103/physrevd.17.2369

Wu, F. Y., Li, X. H., Yang, J. H., & Zheng, Y. F. (2007). Discussions on the Petrogenesis of Granites. *Acta Petrologica Sinica, 23,* 1217-1238. http://www.ysxb.ac.cn/en/article/id/aps_200706118

Wu, H., Li, X. G., Wu, C., Xia, Y., Zhou, Z. X., Xiong, G. Q., & Yao, X. T. (2021). Uranium and Thorium Elements Are Loss in the Deep Inside the Earth?—Disscusion from the Uranium and Thorium Contents of Zircon Minerals from the Caledonian Igneous Plutons in the Qinling Orogen. *Geological Review, 67,* 1207-1230. https://doi.org/10.16509/j.georeview.2021.04.306

Xiong, Q. (2021). Ophiolitic Records of Melt Migration Processes in Oceanic Mantle. *Bulletin of Mineralogy Petrology and Geochemistry, 40,* 999-1011. https://doi.org/10.19658/j.issn.1007-2802.2021.40.043

Xiong, Q., Dai, H., Zheng, J., Griffin, W. L., Zheng, H., Wang, L. et al. (2022). Vertical Depletion of Ophiolitic Mantle Reflects Melt Focusing and Interaction in Sub-Spreading-Center Asthenosphere. *Nature Communications, 13,* Article No. 6956. https://doi.org/10.1038/s41467-022-34781-w

Zhang, G. W., & Zhang, M. K. (2024a). Research on Neutrino Oscillation-Induced Radioactive Decay. *Modern Physics, 14,* 135-144. https://doi.org/10.12677/mp.2024.144016

Zhang, G. W., & Zhang, M. K. (2024b). Dynamics Model of Arch Structure for Basin-Mountain Evolution. *Gansu Geology, 33,* 1-6.

Zhang, G. W. (1999). *The Theory of Neutrino Earth Evolution*. Wuhan University of Surveying and Mapping Technology Press.

Zhang, J., Liu, Y., Foley, S. F., Moynier, F., Zhao, L., Xu, R. et al. (2024). Widespread Two-Layered Melt Structure in the Asthenosphere. *Nature Geoscience, 17,* 472-477. https://doi.org/10.1038/s41561-024-01433-1

Zhang, Q. (2001). *Advanced Heat Transfer*. Xi'an Jiaotong University Press.

Zhao, G., Zhang, J., Yin, C., Wang, C., & Zhang, G. (2023). Pre-Plate Tectonics and Origin of Continents. *Chinese Science Bulletin, 68,* 2312-2323. https://doi.org/10.1360/tb-2022-0249

Zhu, W., Gaetani, G. A., Fusseis, F., Montési, L. G. J., & De Carlo, F. (2011). Microtomography of Partially Molten Rocks: Three-Dimensional Melt Distribution in Mantle Peridotite. *Science, 332,* 88-91. https://doi.org/10.1126/science.1202221